Title: Effect of tool geometry on friction stir processing and fatigue strength of MIG T welds on al alloys

Author: J.S. de Jesus A. Loureiro J.M. Costa J.M. Ferreira

PII: S0924-0136(14)00187-3
DOI: http://dx.doi.org/doi:10.1016/j.jmatprotec.2014.05.012
Reference: PROTEC 13999

To appear in: *Journal of Materials Processing Technology*

Received date: 6-12-2013
Revised date: 8-5-2014
Accepted date: 10-5-2014

Please cite this article as: de Jesus, J.S., Loureiro, A., Costa, J.M., Ferreira, J.M.,Effect of tool geometry on friction stir processing and fatigue strength of MIG T welds on al alloys, *Journal of Materials Processing Technology* (2014), http://dx.doi.org/10.1016/j.jmatprotec.2014.05.012

EFFECT OF TOOL GEOMETRY ON FRICTION STIR PROCESSING AND FATIGUE STRENGTH OF MIG T WELDS ON AL ALLOYS

J.S. de Jesus[1], A. Loureiro[1*], J.M. Costa[1] and J. M. Ferreira[1]

[1]CEMUC, Departamento de Engenharia Mecânica, Faculdade de Ciências e Tecnologia da Universidade de Coimbra,

Rua Luís Reis Santos, Pinhal de Marrocos, 3030-788 Coimbra, Portugal.

* altino.loureiro@dem.uc.pt

Phone number: 00351 239790746

Abstract

Several tool geometries were developed and their effect on weld morphology, material flow, microstructure and hardness of processed regions was analysed. Their effect on fatigue strength of welds was also examined for the most promising tools.The feasibility of FSP MIG T welds was proved. Quality of processed regions is very influenced by tool geometry. FSP removes defects in the MIG weld toe and increases its radius of curvature. Also promotes significant grain refinement in processed regions, reduces hardness in welds on AA 6082-T651 and hardens AA 5083-H111 welds. Only tools with concave and rounded edge shoulder and cylindrical threaded pin allow the improvement of fatigue strength of MIG welds on both alloys.

Highlights

Tool geometry has great influence on properties of FSP MIG welds;

FSP removes defects in the MIG weld toe and increases its radius of curvature;

Grain refinement in processed regions is affected by tool geometry

Tool geometry influences the fatigue strength of FSP MIG T welds.

Keywords

Friction-stir processing; Tool geometry; MIG fillet welds; Aluminium alloys; Fatigue strength.

1. Introduction

Friction stir processing (FSP) is a new technique based on the principles of friction stir welding, developed for microstructural and mechanical modification of metallic materials, as was demonstrated in the past by Devinder et al. (2012) and Karthikeyan et al. (2009). These authors obtained grain refinement and improvement in yield and tensile strengths over the parent material, respectively for processing pure aluminium (99.2 %) and cast aluminum alloy 2285. This microstructural modification results from intense plastic deformation, material mixing and thermal exposure as is described by Ma (2008), all induced by the tool rotation. Indeed, the main functions of the tool are to generate heat by friction and plastic deformation, and to induce material flow in complex paths, by mixing the material in parts to be welded or processed. Early tools for welding and processing consisted of a shoulder and a threaded pin, both cylindrical. But tools with more complex shoulder and pin geometries have subsequently been developed. Concave, flat or convex shoulders with or without scrolls, ridges or knurling, grooves, or concentric circles and cylindrical, conical, oval, triangular pins or pins with more complex geometry, such as whorl or MX triflute pins, for instance, have been developed in recent years, as compiled by Rai et al. (2011). Such complex geometries seek to increase the amount of local heat generated due to the greater interface area between the tool and the workpiece, increasing the flow of material in the stir zone, as mentioned by Mishra et al. (2005). Biswas and Mandal (2011) state that friction is the major contributor to heat generation and concave shoulder and conical pin are preferable to avoid defects in aluminium FSWs, while Leal et al. (2008) concluded that material flow in stir zone of heterogeneous welds in aluminium sheets is very influenced by tool shoulder geometry.. Material flow in the stir zone is very

complex and it is often considered that vertical, straight-through and rotational flows take place around the tool, the material being displaced from the front to the wake of the tool, Reynolds (2008). Some agreement exists with regards to shoulder-driven and pin-driven flows, and the need for good interaction between these flows to obtain defect-free welds Kumar and Kailas (2008). The most suitable tool geometries to reach that interaction are however difficult to predict. For instance, threaded pins are at present the most widely used, even though several researchers, like Lorrain et al. (2010), state that unthreaded pins have the same effect on material flow.

The formation of defects is also influenced by heat generated which increases with the shoulder diameter as was verified by Mehta et al. (2011). Nandan et al. (2008) studied the effect of rotational speed of the tool and concluded that the increase of rotational speed resulted in higher peak temperature. This is beneficial in terms of prevention of defects in stir zone, as confirmed by Kim et al. (2006), but detrimental in terms of microstructure. Indeed, an increase in the heat generated causes the grain growth and reduces the hardness and mechanical strength in the stir zone, as showed Leitão et al. (2009). For this reason, the tool geometry and process parameters must be selected carefully in order to refine the structure and increases mechanical properties in the stir zone. Therefore, this technique can be an alternative to conventional TIG or plasma dressing, Ramalho et al. (2011), or hammering or blasting for instance, Kirkhope et al. (1999), to improve the fatigue behaviour of welded joints. The actual technique is particularly effective for processing fusion welds in aluminium alloys, because they have significant loss of hardness and mechanical strength, which reduces their fatigue strength when compared with the base material. Moreira et al (2007) showed friction stir welds present higher fatigue strength than MIG welds. Els-

Botes et al. (2009) demonstrated the viability of processing MIG/laser butt welds and their fatigue strength improvement with this technique. Friction stir processing of T welds require the development of tools to refine the structure and increase strength of the weld toe, and improve the weld toe radius as well as its surface finish. Tool should also remove previous MIG defects, such as porosity and lack of wetting, without producing other defects, because fatigue life of T welds is reduced considerably by primary crack initiation in the toe due to stress concentration and lower static strength, as demonstrated by Liu et al. (2012). The purpose of this research is to study the feasibility of this process and the effect of tool geometry on friction-stir processing properties of MIG T welds on the aluminium alloys 6082-T651 and 5083-H111. .

2. Experimental procedure

Homogeneous MIG T welds were performed on 6 mm thick plates of 5083-H111 and 6082-T651 aluminium alloys using a SAFMIG TRI 480 welding machine with the torch fixed on an automatic running tracking car. Plates were clamped onto a steel table in order to prevent distortion. The chemical composition and mechanical properties of the base plates are indicated in Tables 1 and 2. The welds were carried out in a flat position using the AWS A5.10-80:ER 5356 filler metal of 1.2 mm diameter and pure argon as shield gas. The joint preparation used in all welds is shown in Figure 1. Two beads were deposited, one in each side, with the parameters listed in Table 3.These parameters, found in preliminary tests, were used for both alloys. The root of the first bead was cleaned with an angle grinder before deposition of the second bead, in order to prevent root defects.

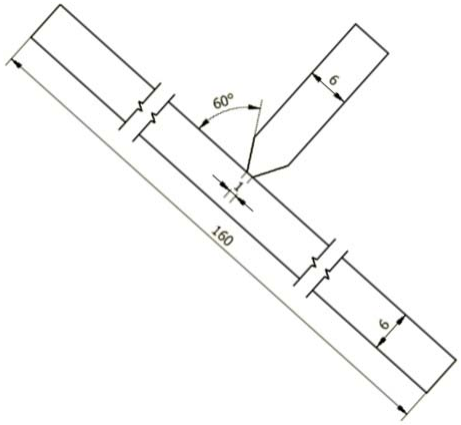

Figure 1 - Joint preparation for MIG welds (dimensions in mm)

Table 1 - Chemical composition of base plates (%wt).

Alloy	Si	Fe	Cu	Mn	Mg	Zn	Ti	Cr	Al
5083-H111	0.4	0.4	0.1	1.0	4.5	0.25	0.15	0.05	Bal.
6082-T651	1.05	0.26	0.04	0.68	0.8	0.02	0.01	0.1	Bal.

Table 2 – Mechanical properties of aluminium alloys.

Alloy	σ_{uts}(MPa)	σ_{tys} (MPa)	ε_{max} (%)	HV
5083-H111	308	158	19.3	80
6082-T651	330	310	10	115

σ_{uts} - Ultimate Tensile Strength; σ_{tys} - Tensile Yield Strength; ε_{max} - Elongation at Break; HV - Vickers hardness.

Table 3 – MIG welding parameters.

Current (A)	Voltage (V)	Speed (cm/min)	Torch distance (mm)
250	24	50	15

The FSP of MIG welds was performed in a Cincinnati milling machine, which allowed control of tool rotational and traverse speeds but not the axial load. For that reason

processing was carried out using a position control strategy, i.e. controlling the plunge depth of the tool. Several tools were developed and tested with the aim of refining the microstructure close to the MIG weld toe and improving the curvature radius in that zone, as well as removing defects typical of MIG welding, such as porosity or lack of wetting. The tool geometries tested are shown in Figure 2. Tools A and B are conventional FSW tools with a concave shoulder and cylindrical threaded pin. The difference between them is that tool A has a sharp edge shoulder unlike tool B whose edge shoulder has a radius of 2.3 mm, as illustrated in Figure 2b. This change was made because tool A makes indents in the weld surface during processing, while welds processed with tool B do not exhibit this defect, as described below. For processing welds on AA 5083-H111, where material flow is difficult as is described by Leitão et al. (2012) for friction stir welds, modifications of tool B, mainly to the radius of curvature in the edge of the shoulder were tested; the radius of curvature at the edge of the shoulder was increased to 3.6 mm in tool D, (Figure 2d) in order to prevent galling in the weld surface, as was observed in welds in this material processed with tool B. Tools C and E, (Figures 2c and 2e), were developed in order to allow processing regions closer to the MIG weld toe. Tool C has a small concave shoulder and a tapered pin with no threads but simple circular grooves with the shape shown in Figure 2c. Tool E has a convex shoulder, to improve access to weld toe, and threaded conical pin, as illustrated in Figure 2e, to promote material flow towards the bottom of processed region. All these tools were manufactured in quenched and tempered steel AISI H13, with an average hardness of 50-52 HRC.

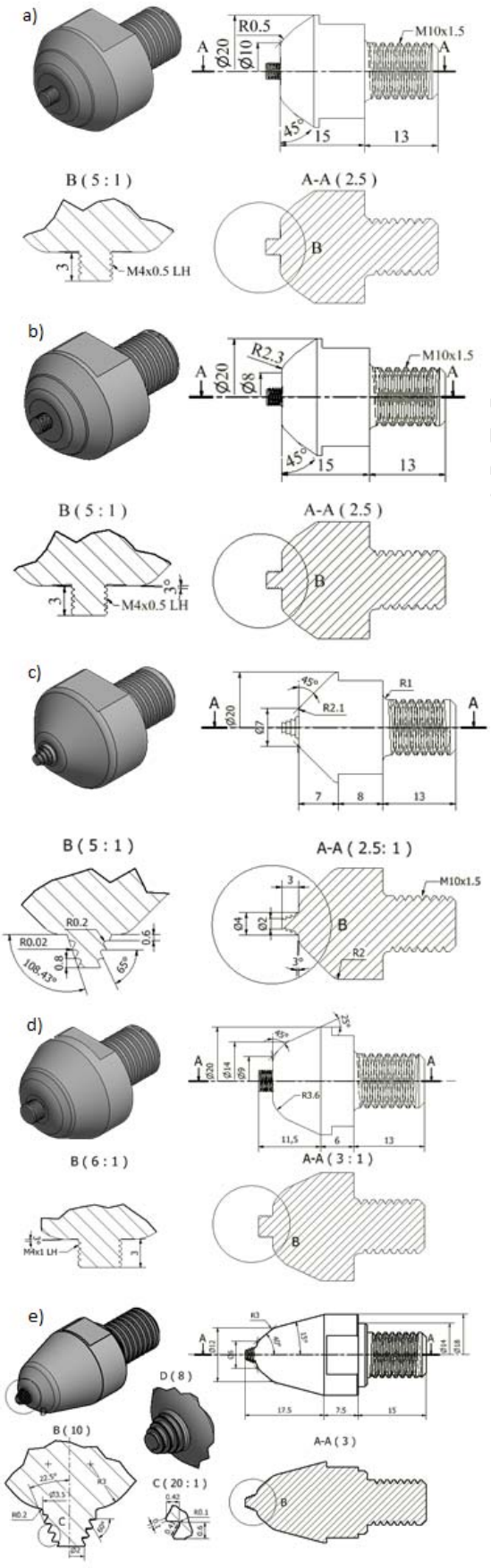

Figure 2 – Geometries of the tools developed and tested: a) Tool A; b) Tool B; c) Tool C; d)Tool D (dimensions in mm)

The mode of operation of the tools A, B and D is illustrated in Figure 3. The tools were positioned so as to interfere with the horizontal weld toe for a distance of approximately 0.5 mm and using a penetration depth of 3 mm.

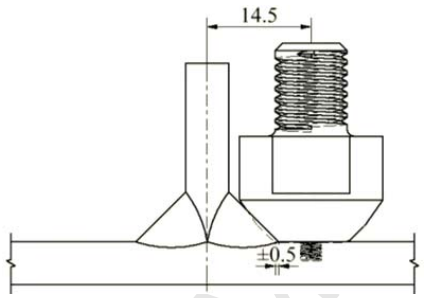

Figure 3 – Mode of operation of tools A and B and D (dimensions in mm).

The placement of the tools C and E is shown in Figure 4.

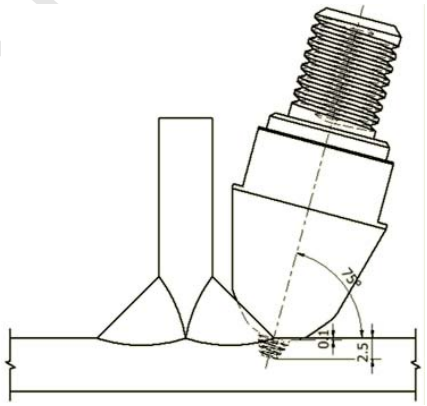

Figure 4 – Mode of operation of tool C and E (dimensions in mm).

In addition to the angle of 75^0, shown in the image, a tool tilt angle of 13^0 in the processing direction was used for these tools, in order to constrain the flow of material in stir zone, preventing the formation of flash and cavities. A penetration depth of 2.5 mm was used. Tool design and positioning resulted from a theoretical study using CAD software and experimental work. The processing parameters for the different materials and tools are indicated in table 4. These parameters were chosen based on previous tests. For the same rotational speed a lower traverse speed was required to prevent the formation of voids in the stir zone on AA 5083-H111.

Table 4 – Friction Stir Processing parameters.

Alloy	Tool	ω(rpm)	v (mm/min)	N*	TA (^{0})
6082-T651	A, B	1500	240	2	2.5
	E	1500	240	2	13
5083-H111	D	1500	120	2	2.5
	C and E	1500	120	2	13

ω - Rotation speed; v – Traverse speed; N – number of passages; * - One in each side; TA – Tilt angle.

The geometry of weld toes before and after processing was characterized by the curvature radius (ρ) and the angle (θ), as illustrated in Figure 5. These data were obtained from images of cross sections of the welds obtained in a profile projector, and measured with the Autodesk Inventor software. In addition surface finish of processed region in the weld toe was characterized by the average roughness (Ra) measured in a Mitutoyo Surftest-SJ-500/P Series 178 roughness meter. Metallographic specimens were removed transversely to the welding direction from unprocessed and processed welds, polished according to standard practice and etched with Poulton's reagent for 5 s. Grain size was measured using ASTM E 112 – 96e2 intercept procedure. Vickers hardness profiles were measured at the cross section of the welds,

with a load of 0.2 kgf for 15 s, according to the ASTM E 348 standard, using a Struers Type Duramin-1 microhardness tester. Measurements were taken along a line located 0.25 mm below the surface of the horizontal plate at distances between indents of 0.5 mm.

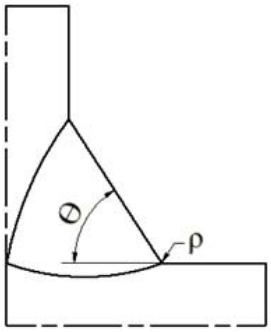

Figure 5 – Parameters used to characterize the weld toe geometry.

The fatigue tests were carried out using an Instron hydraulic machine, loading the specimens perpendicular to the weld bead direction, applying a constant amplitude sinusoidal load wave with a frequency within the range 20-30 Hz, a stress ratio set at R=0 and stress ranges between 90 and 170 MPa.

3. Results and discussion

3.1 *Morphology of unprocessed and processed welds*

MIG welds showed excellent visual appearance without any defects and with regular geometry, as illustrated in Figure 6, for a welding performed on alloy 5083-H111. Processing induced a significant change in the geometry of the welds, especially in the weld toe, as illustrated in the image for the same weld processed with tool D. The change in the weld toe geometry induced by the different tools, characterized by ρ

and θ, is indicated in table 5. This table shows that, with the exception of tool A, the other tools produce a significant increase in the toe radius for both materials. The small increase in toe radius given by tool A is related to its shoulder sharp edge geometry. With regard to the angle θ it is influenced not only by the geometry of the tool but also by the position in which it works. Tools A, B and D reduce the θ angle while tool E increases this angle. Tool C was not used in subsequent tests because it produced cavities in the processed region (see below). The tool geometry affects also the surface finish of processed region as can be seen in the same table by comparing Ra of welds processed with tools B or D with those processed with tool E. This difference is related with the higher contact area between the convex shoulder and the weld given by tool E. Roughness is affected by the base material too; processed regions in AA 6082-T651 have higher average roughness than those in AA5083-H111, see in table 5, suggesting different contact conditions between the tool and the material.

An important effect of FSP is that leads to a significant reduction of the distortion caused by MIG welding, due to the plastic strain introduced during processing.

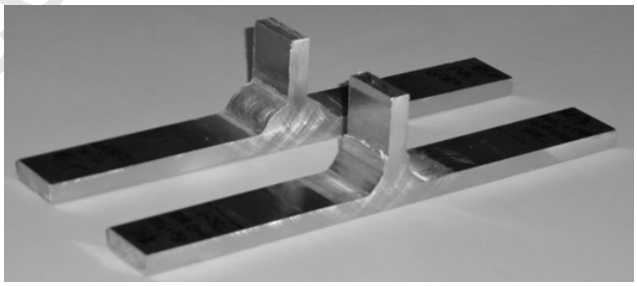

Figure 6 – Surface appearance of an unprocessed and processed weld on AA 5083-H111 (tool D).

Table 5 – Geometry of unprocessed and processed weld toes.

AA6082-T651			
	ρ(mm)	Θ (º)	Ra (μm)
MIG	0,6	58,2	-
MIG+FSP_tool A	0,7	45,9	-
MIG+FSP_tool B	2,3	45,3	5.64
MIG+FSP_tool E	3,9	66,2	10.31
AA5083-H111			
	ρ(mm)	Θ (º)	Ra (μm)
MIG	0,4	54,8	-
MIG+FSP_tool D	3,5	45,1	1.82
MIG+FSP_tool E	4,2	65,3	5.32

3.2. *Microstructure of MIG welds*

Macroscopic analysis of MIG welds on both alloys, AA 6082-T651 and 5083-H111, revealed good weld penetration depth and little porosity as well as apparently good wetting of both base materials, as illustrated in Figure 7.The microstructures of base materials and MIG welds close the toe are also shown in the same image. The microstructure of the AA 6082-T651 consists of grains elongated in the rolling direction with grain size of 135-150 μm and 80-90 μm, on rolling and thickness directions, respectively, as shown in Figure 7.1a), unlike the AA 5083-H111 which has grains only slightly elongated in the rolling direction with an average grain size of 25 to 35 μm, as illustrated in Figure 7.2a).

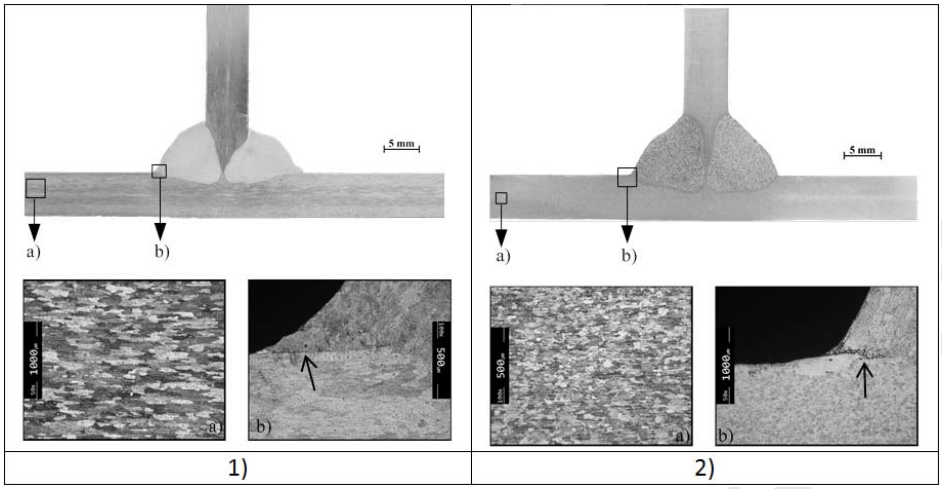

Figure 7 – Macrographs and micrographs of MIG welds made on aluminium alloys: 1) a) AA 6082-T651 microstructure; b) Weld toe; 2) a) 5083-H111 microstructure; b) Weld toe.

The microstructure in the toe of MIG welds on alloy AA6082-T651 consists of coarsened grains elongated in the heat flow direction, and shows some porosity and lack of wetting, indicated by an arrow in Figure 7.1b),. Welds performed on AA 5083-H111 display coarsened structure in the melted region and occasionally a slight lack of wetting, as shown in Figure 7.2b). The coarsened structures and defects in that region have in general a very detrimental effect on the fatigue strength of welded joints, because they promote fatigue crack initiation.

3.3. *Microstructure of processed welds*

Welds on AA 6082-T651

The region processed with tool A on MIG welds on AA6082-T651 is at a significant distance from the MIG weld toe, see Figure 8.1, suggesting that the material in this zone was not practically processed. However, Figure 8.2 shows that a thin layer of

material was processed in the weld toe, and the lack of wetting of MIG welds was removed. However the same image shows that this tool makes stretch marks on the surface of the processed region, caused by the sharp edge of tool A. Although these marks are small, preliminary fatigue tests showed that they are starting points for fatigue crack initiation. Therefore this tool was not subsequently used in the processing of welds.

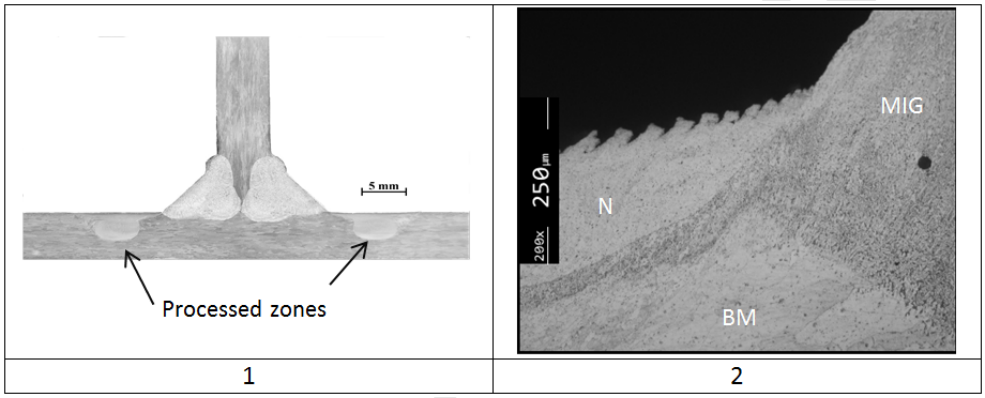

Figure 8– MIG weld made on AA 6082-T651 and processed with Tool A; 1) Macrograph; 2) Micrograph in the toe region.

Most of the area processed by tool B is also at a significant distance from the MIG weld toe, see Figure 9.1 but, unlike tool A, tool B gives smooth processed zones without stretch marks, (See Figure 9.4.). However tool B, like tool A, processes only the surface layer at the weld toe, removing the issue of lack of wetting. This image also shows the increase in the radius of curvature reached in the weld toe (2.3 mm) when this tool is used. The material flow in the stir zone influences the formation of defects in that zone. Shoulder driven and pin driven flows have been detected in the stir zones (SZs) processed with this tool, as illustrated in Figure 9.2, the transition between the nugget (N) and the TMAZ being more abrupt in the advancing side than in the

retreating side, as can be observed by comparing Figures 9.2 and 9.3. During initial tests the formation of voids was verified in the advancing side, in the region of interaction between the shoulder driven (SD) and pin driven (PD) flows of material. This region is marked with an arrow in Figure 9.2. In our opinion these defects form because of insufficient material flow dragged by the tool which may be caused by insufficient heat input and/or low axial load. In this case the low plunge depth could be identified as the cause, because high rotational speed and low traverse speed were used in FSP. Indeed, increasing the plunge depth causes voids to disappear from the stir zone. However, plunge depth must be combined with the interference between tool shoulder and MIG weld, in order to prevent unwanted changes in the final geometry of the weld. As in regions processed with tool A, the stir zone processed with tool B shows substantial grain refinement when compared with the base material, of about 4-6 μm. It is therefore concluded that it is not desirable to use a sharp shoulder edge in this tool geometry.

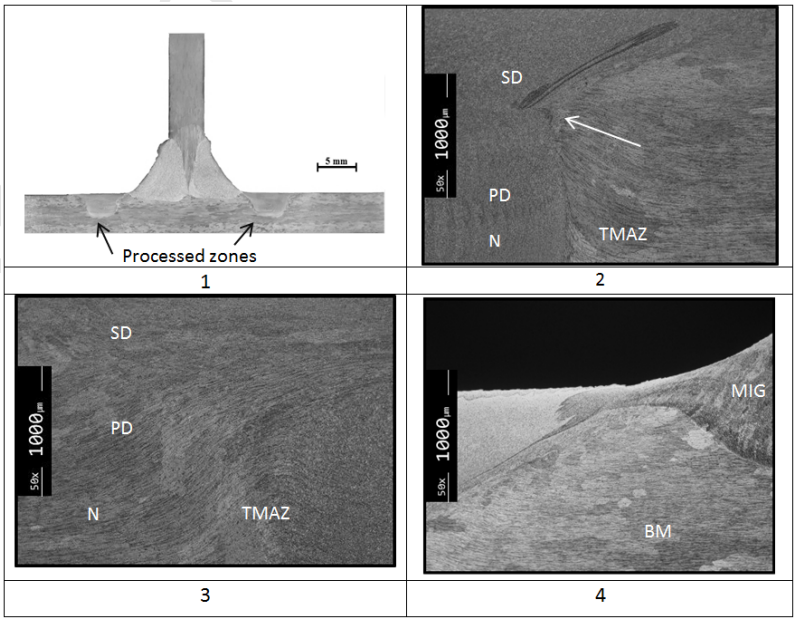

Figure 9– MIG weld made on AA 6082-T651 and processed with Tool B; 1) Macrograph; 2) Advancing side of stir zone; 3) Retreating side of stir zone; 4) Toe region. N – Nugget; TMAZ – Thermomechanically affected zone; PD – pin driven flow; SD – shoulder driven flow.

Tool E was developed to provide the tool pin with access to the weld toe, without damaging the profile of the MIG welds. In addition to the change in the tool profile it was still necessary to change its tilt angle, so as to ensure an adequate pressure in the zone being processed, in order to prevent the formation of internal voids. With this tool, the processed area was focused exactly at the toe of the MIG welds, as illustrated in Figure 10.1. This image also shows that although the radius of curvature in the weld toe was increased (to 3.9 mm), tool E produced some reduction in plate thickness, which is detrimental in terms of fatigue strength. Material flow in the SZ is difficult to evaluate because microstructure is very refined and homogeneous although the upward material flow is suggested by the deformation of the non-recrystallized grains in the advancing side, (see Figure 10.2). Figure 10.3 shows that the transition between recrystallized and non-recrystallized regions is smoother in the retreating side. Figure 10.4 shows greater refinement of the structure in the stir zone as well as increasing radius of curvature at the weld toe, as mentioned above. The grain size in the nugget is about 8-12 μm, greater than that made by the tool B, suggesting greater heat generated by this tool. As tool rotation and traverse speeds are the same as tool B, the increase in heat generated should be justified by the increased area of interaction between the tool shoulder and the aluminium plate, producing more friction heat.

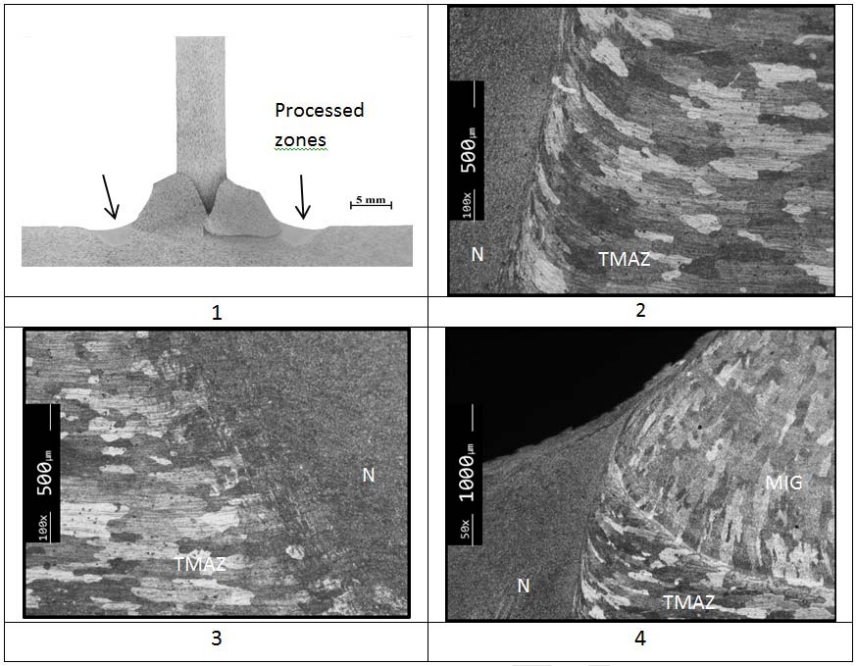

Figure 10– MIG weld made on AA 6082-T651 and processed with Tool E; 1) Macrograph; 2) Advancing side of stir zone; 3) Retreating side of stir zone; 4) Toe region.

Welds on AA 5083-H111

The processing of the welds on AA 5083-H111 was performed with tools C, D and E using the same welding parameters used on AA 6082-T651, except for traverse speed, which was only half that previously used. As FS processing on that alloy seemed to form tunnel defects a low traverse speed was applied in order to prevent these defects. These parameters were chosen based on experimental tests. The reason for that change is the different behaviour of both alloys when plastically deformed at high temperature, as demonstrated by Leitão et al (2012). These authors mention that the alloy 5083-H111 shows a lower reduction of mechanical strength with increasing

temperature than the alloy 6082-T651, which makes plastic flow of the material more difficult during FS welding or processing. This difference of performance between the two alloys justifies the observed differences between processed areas in both materials. For example, for the welds processed with tool D the thickness of the layer processed in the MIG weld toe is smaller for AA5083-H111 than for AA6082-T651, processed with tool B, which is quite similar to tool D, as can be seen by comparing Figures 9.4 and 11.4. Although the volume of material dragged by the tool is smaller for AA 5083-H111 than for AA 6082-T651 the transition between the nugget and TMAZ is very obvious, either in the advancing or retreating sides, as illustrated in Figures 11.2 and 11.3. An important grain refinement was also reached in the nugget (average grain size about 2-4 μm), as shown in the same images.

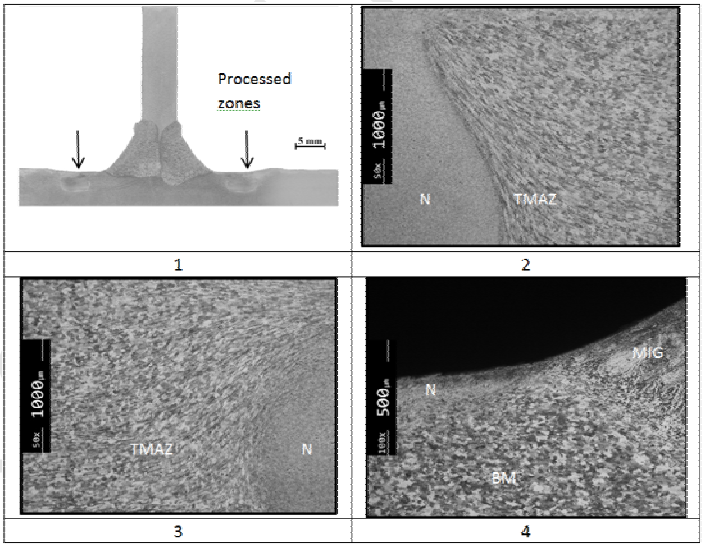

Figure 11– MIG welds made on AA 5083-H111 and processed with Tool D: 1) Macrograph; 2) Advancing side of stir zone; 3) Retreating side of stir zone; 4) Toe region.

Processing performed on this alloy using tool E placed the processed region in the weld toe, but introduced a reduction of plate thickness, (see Figure 12.1), as in the weld performed with the same tool on AA6082-T6. However, the flow of material in the nugget is different from that of the latter alloy. In fact the flow of material in the AA 5083-H111 occurred in horizontal layers, mainly in the top close to the weld toe, as shown in the Figure 12.2, for the advancing side of processing. This morphology is related with material properties and process parameters because it was not observed for processing with the same tool on AA 6082-T651, (see Figure 10.). Also grain refinement occurs in the nugget, as illustrated in Figure 12.3, but the grain size (8-10 μm) is greater than that obtained with tool D (2-4 μm). As the processing parameters are the same this grain coarsening is related to higher friction heat generated by tool E.

Tool C, which has no thread but only toothed rings, produced a similar material flow, (see Figure 12.4), but showed a tendency to produce small defects between layers, as shown by an arrow in the image. This suggests that the tool does not induce material flow in the direction of plate thickness, increasing the probability of formation of cavities. For this reason the tool was not used in subsequent trials.

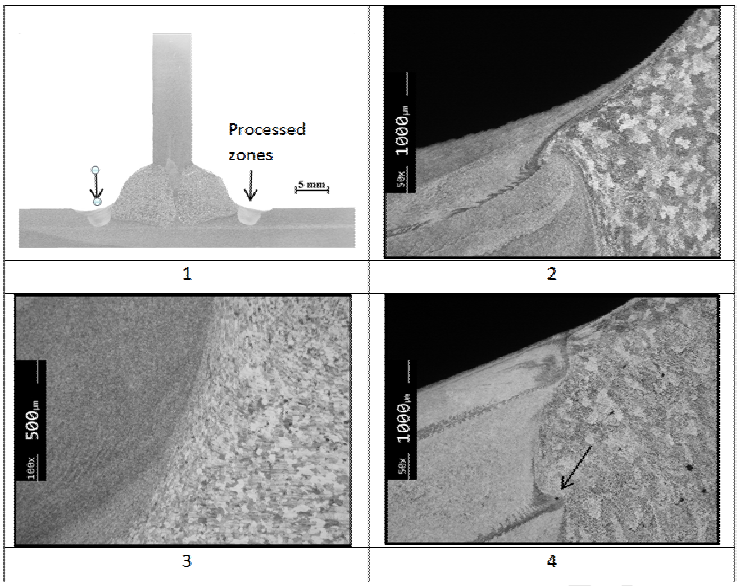

Figure 12– MIG welds made on AA 5083-H111 and processed with: Tool E, 1) Macrograph; 2) Toe region; 3) Nugget; and 4) with tool C: Toe region.

3.4. *Hardness profiles*

AA 6082-T651

The hardness distribution in the cross section of the MIG welds performed on alloy 6082-T651 is illustrated in Figure 13. A substantial hardness reduction (about 35% when compared with base material) was observed in melted and heat-affected zones, due to filler metal composition as well as to dissolution and coarsening of strengthening precipitates, as mentioned by several authors among which Olea et al. (2007) for 6XXX alloys in T6 condition. Currently the loss of hardness is accompanied by loss of mechanical strength in these alloys, El-Danaf, 2013. The loss of hardness is more pronounced precisely in the heat-affected zones, located in one and the other side of the welds, roughly at 8 mm from the centre of the joint.

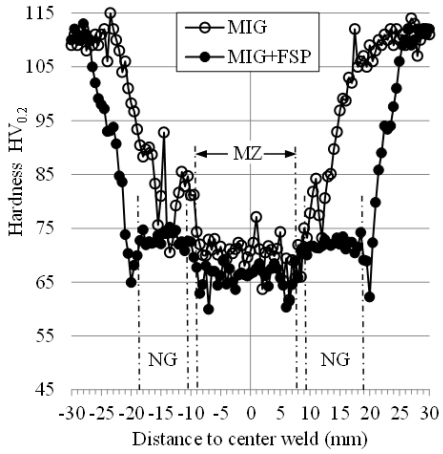

Figure 13- Hardness profiles of unprocessed (MIG series) and processed (MIG+FSP series) welds with tool B, both on AA6082-T651.

The same image also shows the hardness profile of the weld processed with tool B. The most noticeable effect of processing was the enlargement of the zone where there is loss of hardness. The stir zone in each side of MIG welds displays hardness similar to that of the melted material before processing while the melted zone exhibits a slight decrease in hardness after processing, certainly due to coarsening of strengthening precipitates. The same effect can explain the greater decrease in hardness in the thermomechanically affected zones in both sides of processed layers. The hardness profile of a weld processed with tool E is shown in Figure 14.

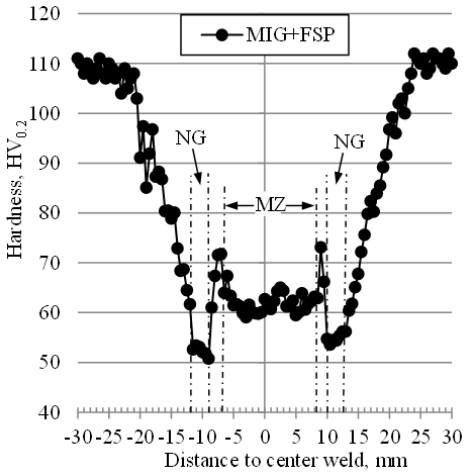

Figure 14- Hardness profile of a processed (MIG+FSP series) weld with tool E, on AA 6082-T651.

As processing was performed exactly at the weld toe, the width of the weld zone where there is loss of hardness is smaller than in welds processed with tool B, but the loss of hardness is greater. This may also be caused by a higher aging of welds, suggesting once more that tool E generates more heat than tool B. However, the greater proximity between the processed zones and MIG welds may also contribute to this effect, though this does not explain the reduced hardness of the stir zones.

AA 5083-H111

MIG welds performed on alloy 5083-H111 showed a small reduction in hardness, in the order of 15%, in the weld metal and heat affected zones when compared with the base material, as shown in Figure 15.

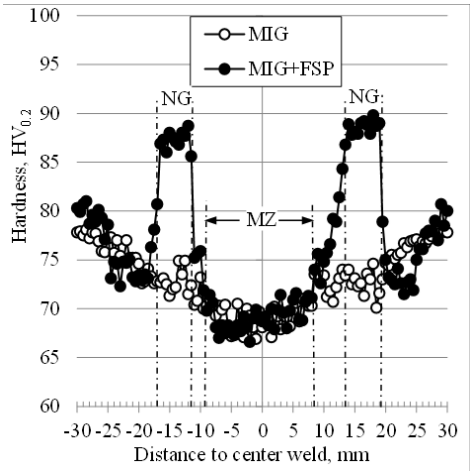

Figure 15- Hardness profiles of unprocessed (MIG series) and processed (MIG+FSP series) welds with tool D, both on AA 5083-H111.

Friction stir processing with tool D produced only a slight increase in hardness in stir zones, in the order of 10% of base metal, as illustrated in the same image, mainly due to grain refinement in those zones and plastic deformation in thermomechanically affected zones. This hardening is common for FS welds in this alloy, especially when it is in soft condition, as mentioned by Fuller et al. (2006). A small softening can also be observed in heat affected zones of processed layers, due to annealing of the base material.

The welds processed with tool E have a hardness profile similar to that achieved with tool D, see Figure 16, but exhibit somewhat greater hardness in processed zones. This small increase in hardness is due to some residual plastic deformation caused by the tool shoulder, instead of larger grain refinement, because grain size is larger in stir zones processed by tool E. Furthermore there is another important difference between the effects of the two tools: tool D produces an increase in hardness at points some distance from the weld toe while tool E produces the increase in hardness exactly in

the weld toe. Moreover, the heat affected zones, adjacent to the processed zones, are wider in the case of welds processed with tool E, which also confirms that more heat is generated by this tool.

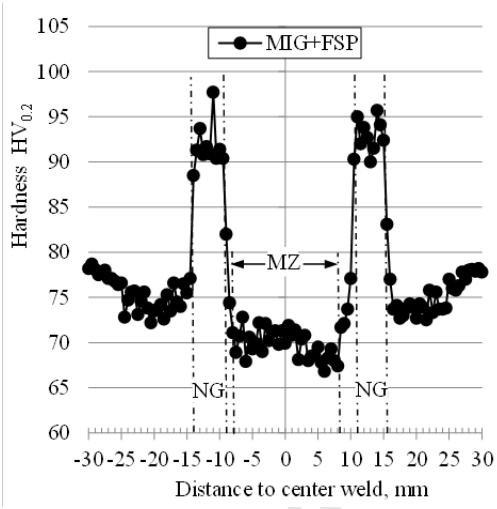

Figure 16- Hardness profile of a processed (MIG+FSP series) weld with tool E, on AA 5083-H111.

3.5. *Fatigue strength*

The feasibility of friction stir processing of MIG fillet welds is therefore demonstrated although proof is lacking as to whether the processing has an effect in terms of the fatigue performance of welds. Figure 17 presents the fatigue results for the processed and unprocessed welded specimen series and base material AA 6082-T651, plotting the nominal stress range against the number of cycles to failure. MIG weld series have a substantial decrease in fatigue strength relative to the base material, because of the decrease in hardness and mechanical strength in the weld toe as well as the local stress concentration caused by the small curvature radius and other

defects mentioned above. The effect of residual stress was not evaluated at this stage. The fatigue crack initiated at the toe for all welds, as illustrated in Figure 18. Figure 17 also shows that weld series processed with tool B have a significant increase in fatigue strength; for a life of 10^6 cycles fatigue strength increased from 100 MPa to 130 MPa. As demonstrated above, the increase in fatigue strength of MIG welds on AA 6082-T651 cannot be explained by the increase in mechanical strength, but by the microstructural change (grain refinement), the removal of previous defects (porosity and lack of wetting) as well as increased weld toe radius and better surface finish. Unlike the weld series processed with tool E, there is no increase in fatigue strength, and it may even be lower than the MIG series. The reason for this is related to the thickness reduction induced by the tool, as shown in Figure 10.1.This reduction contributes in two ways to the reduction in fatigue strength: it increases the average stress and acts as a local stress concentrator. Besides the surface finish given by tool E is worse than that achieved with the tool B.

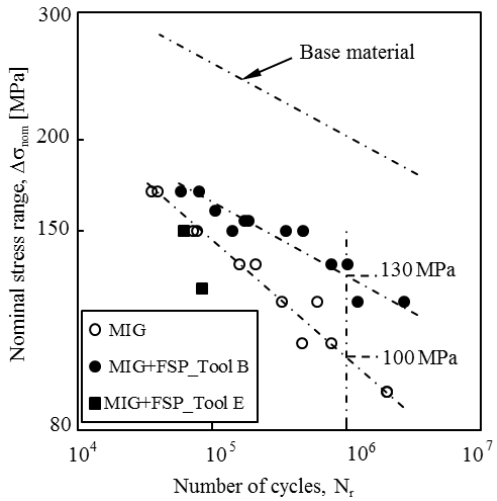

Figure 17 -Results of fatigue tests: nominal stress range versus number of cycles to failure for AA 6082-T651 and unprocessed and processed welds.

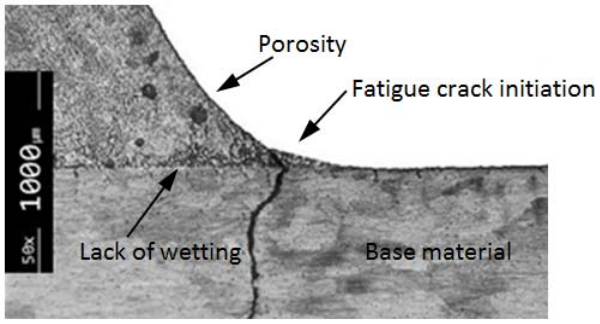

Figure 18 – Fatigue crack initiation site on a MIG weld (AA 6082-T651).

The effect of the MIG welding on AA 5083-H111 is identical to that observed in AA 6082-T651, a reduction in fatigue strength, as shown in Figure 19. Processing of MIG weld with tool D also provided increased fatigue strength, for instance from 114 MPa to 149 MPa for a fatigue life of 10^6 cycles, (see the same image). This increase is due not only to those factors mentioned above (removal of defects, grain refinement and improved toe geometry) but also to increased mechanical strength at the weld toe, as demonstrated by the hardness increase in Figure 14.The processing with tool E of MIG welding on AA 5083-H111, as in AA 6082-T651, produces no increase in fatigue strength, suggesting that this tool geometry is not adequate or tool tilt angles during processing must be changed, in order to prevent thickness reduction.

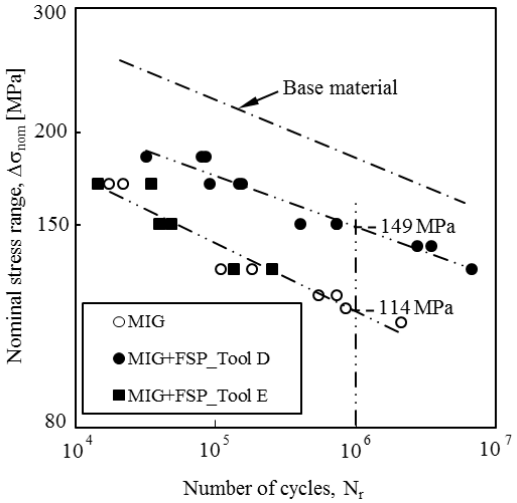

Figure 19 - Results of fatigue tests: nominal stress range versus number of cycles to failure for AA 5083-H111 and unprocessed and processed welds.

4. Conclusions

The following conclusions were drawn:

- The feasibility of friction-stir processing MIG T welds, using tools with concave shoulder geometry has been demonstrated;
- Tools with convex shoulder geometry allow the placement of the nugget on the MIG weld toe but cause weld defects such as cavities or reduction in plate thickness;
- Friction stir processing causes significant grain refinement in the nugget in both alloys studied and removes defects, such as pores and lack of wetting, pre-existing in the MIG weld toe;
- Friction stir processing with concave shoulder tools increases the fatigue strength of MIG welds carried out either on AA 6082-T651 or AA 5083-H111.

Acknowledgements

The authors gratefully acknowledge the Portuguese Foundation for Science and Technology for funding this study , Project nº PTDC/EME-PME/114605/2009 co-financed by FEDER, through the Operational Factors for Competitiveness

This research is sponsored by FEDER funds through the program COMPETE – Programa Operacional Factores de Competitividade – and by national funds through FCT – Fundação para a Ciência e a Tecnologia –, under the project PEst-C/EME/UI0285/2013

This research is also sponsored by FEDER funds through the program COMPETE – Programa Operacional Factores de Competitividade, under the project CENTRO -07-0224 -FEDER -002001 (MT4MOBI)

The authors thank Thyssenkrupp Portugal - Steels and Services Ltd., Marinha Grande, for providing heat treatments of friction stir processing tools developed.

References

Biswas P., Mandal N.R.,2011. Effect of tool geometries on thermal history of FSW of AA1100, Supp. to Welding J. 90, 129-136.

Devinder Y., Ranjit B., 2012. Effect of friction stir processing on microstructure and mechanical properties of aluminium. Mater. Sci. Eng. A. 539, 85–92.

El-Danaf, E. A., El-Rayes, M. M., 2013, Microstructure and mechanical properties of friction stir welded 6082 AA in as welded and post weld heat treated conditions,

Mater. Des. 46, 561-572.

Els-Botes, A.; Hattingh, D.G.; Mjali, K.V., 2009. The effect of Friction Stir Processing on the fatigue life of MIG-Laser hybrid welded joints as compared to conventional FSW 6082-T6 aluminium joints, Surface Effects and Contact Mechanics IX, Book Series: WIT Transactions on Engineering Sciences, Ed: DeHosson, J.T.M; Brebbia, CA, 183-193.

Fuller C. B., 2007. Friction Stir Tooling: Tool Materials and Designs, In: Rajiv S. Mishra, Murray W. Mahoney, Proceedings of Fiction Stir Welding and Processing, ASM International, 7-36.

Fuller C.B., Mahoney W.M., 2006. The Effect of Friction Stir Processing on 5083-H321/5356 Al Arc Welds: Microstructural and Mechanical Analysis, Metall. Mater. Trans A 37A, 3605-3615.

Karthikeyan L., Senthilkumar V.S., Balasubramanian V., Natarajan S., 2007. Mechanical property and microstructural changes during friction stir processing of cast aluminum 2285 alloy. Mater. Des. 48, 169-177.

Kim Y.G., Fujii H., Tsumura T., Komazaki T., Nakata K.,2006. Three defect types in friction stir welding of aluminum die casting alloy, Mater. Sci. Eng. A 415, 250-254.

Kirkhope K.J., Bell R., Caron L., Basu R.I., Ma K.T, 1999. Weld detail fatigue life improvement techniques. Part 2: application to ship structures. Marine Structures 12, 477-496.

Kumar K, Kailas SV, 2008. The role of friction stir welding tool on material flow and

weld formation. Mater Sci Eng, A 485, 367–374.

Leal R.M., Leitão C., Loureiro A., Rodrigues D.M., Vilaça P., 2008. Material Flow in Heterogeneous Friction Stir Welding of Thin Aluminium Sheets: Effect of shoulder geometry. Mat. Sci. Eng. A 498, 384-391.

Leitão C., Leal R.M., Rodrigues D.M., Loureiro A., Vilaça P., 2009. Mechanical behaviour of similar and dissimilar AA5182-H111 and AA6016-T4 thin friction stir welds. Mater. Des. 30, 101-108.

Leitão C., Louro R., Rodrigues D.M., 2012. Analysis of high temperature plastic behaviour and its relation with weldability in friction stir welding for aluminium alloys AA5083-H111 and AA6082-T6. Mater. Des. 37, 402-409.

Liu X.S., Wang P., Yan Z.J., Wang Q., Fang H.Y., 2012. Geometric parameters optimization design for aluminium alloy welding joint based on increasing fatigue strength Physical and Numerical Simulation of Material Processing VI, pts 1 and 2 Book Series: Materials Science Forum. 704-705, 1106-1111.

Lorrain O., Favier V., Zahrouni H., Lawrjaniec D., 2010. Understanding the material flow path of friction stir welding process using threaded tools, J. Mater. Process. Tech. 210, 603-609.

Ma Z.Y., 2008. Friction Stir Processing Technology: A Review. Metall. Mater. Trans. A 39 A , 642-658.

Mehta M., Arora A., De A., DebRoy T.,2011. Tool Geometry for Friction Stir Welding – Optimum Shoulder Diameter. Metall. Mater. Trans. A 42, 2716-2722.

Mishra R.S., Ma Z.Y., 2005. Friction stir welding and processing, Materials Science and Engineering. R 50, 1–78.

Moreira P.M.G.P, de Figueiredo M.A.V., de Castro P.M.S.T., 2007. Fatigue behaviour of FSW and MIG weldments for two aluminium alloys. Theor. Appl. Fract. Mec. 48, 169–177.

Nandan R., DebRoy T., Bhadeshia H.K.D.H., 2008. Recent advances in friction-stir welding – Process, weldment structure and properties. Prog. Mater. Sci.53, 980-1023.

Olea C.A.W., Roldo L., dos Santos J.F., Strohaecker T.R., 2007. A sub-structural analysis of friction stir welded joints in an AA6056 Al-alloy in T4 and T6 temper conditions, Mater. Sci. Eng. A 454-455, 52-62.

Rai R., De A., Bhadeshia H.K.D.H., DebRoy T., 2011 review: friction stir welding tools, Sc. Techn. Wel.& J. 16-4, 325-342.

Ramalho A., Ferreira J.A.M., Branco C.M., 2011. Fatigue Behaviour of T Welded Joints Rehabilitated by Tungsten Inert Gas and Plasma Dressing, Mater. Des. 32, 4705-4713.

Reynolds A.P., 2008. Flow visualization and simulation in FSW. Scripta Mater. 58, 338-342.

Figure captions

Figure 1 - Joint preparation for MIG welds (dimensions in mm)

Figure 2 – Geometries of the tools developed and tested: a) Tool A; b) Tool B; c) Tool C; d)Tool D (dimensions in mm).

Figure 3 – Mode of operation of tools A and B and D (dimensions in mm).

Figure 4 – Mode of operation of tool C and E (dimensions in mm).

Figure 5 – Parameters used to characterize the weld toe geometry.

Figure 6 – Surface appearance of an unprocessed and processed weld on AA 5083-H111 (tool D).

Figure 7 – Macrographs and micrographs of MIG welds made on aluminium alloys: 1) a) AA 6082-T651 microstructure; b) Weld toe; 2) a) 5083-H111 microstructure; b) Weld toe.

Figure 8– MIG weld made on AA 6082-T6 and processed with Tool A; 1) Macrograph; 2) Micrograph in the toe region.

Figure 9– MIG weld made on AA 6082-T651 and processed with Tool B; 1) Macrograph; 2) Advancing side of stir zone; 3) Retreating side of stir zone; 4) Toe region. N – Nugget; TMAZ – Thermomechanically affected zone; PD – pin driven flow; SD – shoulder driven flow.

Figure 10– MIG weld made on AA 6082-T651 and processed with Tool E; 1) Macrograph; 2) Advancing side of stir zone; 3) Retreating side of stir zone; 4) Toe region.

Figure 11– MIG welds made on AA 5083-H111 and processed with Tool D: 1) Macrograph; 2) Advancing side of stir zone; 3) Retreating side of stir zone; 4) Toe region.

Figure 12– MIG welds made on AA 5083-H111 and processed with: Tool E, 1) Macrograph; 2) Toe region; 3) Nugget; and 4) with tool C: Toe region.

Figure 13- Hardness profiles of unprocessed (MIG series) and processed (MIG+FSP series) welds with tool B, both on AA6082-T651.

Figure 14- Hardness profile of a processed (MIG+FSP series) weld with tool E, on AA 6082-T651.

Figure 15- Hardness profiles of unprocessed (MIG series) and processed (MIG+FSP series) welds with tool D, both on AA 5083-H111.

Figure 16- Hardness profile of a processed (MIG+FSP series) weld with tool E, on AA 5083-H111.

Figure 17 -Results of fatigue tests: nominal stress range versus number of cycles to failure for AA 6082-T651 and unprocessed and processed welds.

Figure 18 – Fatigue crack initiation site on a MIG weld.

Figure 19 - Results of fatigue tests: nominal stress range versus number of cycles to failure for AA 5083-H111 and unprocessed and processed welds.

Table captions

Table 1 - Chemical composition of base plates (%wt).

Table 2 – Mechanical properties of aluminium alloys.

Table 3 – MIG welding parameters.

Table 4 – Friction Stir Processing parameters.

Table 5 – Geometry of unprocessed and processed weld toes.